富山大学水素同位体科学研究センター研究報告28：9－22，2008.

Preliminary Study of H_2O Adsorption on Cr_2O_3 and Al_2O_3 Surfaces by *Ab Initio* Cluster Calculations

K. Watanabe, Y. Torikai, M. Hara and Y. Hatano
Hydrogen Isotope Research Center, University of Toyama
Gofuku 3190, Toyama 930-8555, Japan
(Received Dec. 26th, 2008: Accepted Feb. 23th, 2009)

ABSTRACT

Adsorption and desorption of water over Cr-oxide and alumina are of great concern with the contamination of stainless steel and gas chromatographic isotope separation. However, the mechanisms of those phenomena have not been fully clarified. A preliminary *ab inito* study on the behavior of water molecules on the (001) surfaces of α-Cr_2O_3 and α-Al_2O_3 was carried out for small clusters of Me4O4 (Me = Cr or Al) by use of the Gaussian 03 package.

It was found that water molecules can be adsorbed molecularly and dissociatively on these surfaces. Molecular adsorption of a H_2O molecule takes place on a metal atom of the cluster as Me-OH_2, with the bond length of about 2.0 Å. Dissociative adsorption occurs by forming Me-OH (on-top site) or Mc2-OH (bridge site) and O-H bonds. There appeared a feature that the bond length of Me2-OH is greater than that of Me-OH.

Calculated adsorption energies were examined by comparing with the values estimated from the thermal desorption spectra of water for α-Cr_2O_3 and γ-alumina. The *ab initio* calculations coincided quite well with the observed thermal desorption spectrum for α-Cr_2O_3, whereas they did not for γ-alumina. Further studies are required to clarify the structures of adsorbed species, adsorption energies and kinetic processes.

1. Introduction

Adsorption of water vapor on oxides such as Cr_2O_3 and Al_2O_3 is an important problem to develop tritium-handling techniques. The former is concerned with tritium handling systems, where stainless steel such as SS316 is commonly used as structural material. Since the surface of stainless steel is usually covered with native oxides such as Cr_2O_3[1, 2], behavior of water on Cr_2O_3 surface is of great importance for tritium contamination and decontamination. The latter, Al_2O_3, has been used for gas chromatic separation of hydrogen isotopes as a support material of the working material such as Pd and/or Pd-Pt alloy particles[3, 4]. Adsorption of water vapor significantly affects the performance of the isotope separation[5, 6].

As for the tritium-contamination of stainless steel, it has been revealed that the contamination can be divided into two types: one is the tritium solution in the bulk and the other tritium capturing by a thin sub-surface layer[7, 8]. It should be noticed that the tritium concentration in the sub-surface layer is considerably higher than that in the bulk[7, 8, 9]. It was also found that tritium captured in the bulk can be released rather easily to gas phase by heating in vacuum and/or in inert gas atmosphere, whereas the removal of tritium captured

by the sub-surface layer is much more difficult[7, 8]. The tritium in the bulk is attributed to tritium solved in the interstitial site of the bulk structure. As for the tritium captured in the sub-surface layer, it is considered to be the one captured in the native oxide layer of stainless steel comprising Cr_2O_3[7, 8]. From these viewpoints, extensive studies of the contamination and decontamination of the stainless steel have been carried out but no further details of capturing by the sub-surface layer have not been clarified so far. For example, it should be mentioned here that tritium is predominantly released as elemental form, HT, to gas phase under evalulation, whereas it is essentially in the form of HTO in inert gas atmosphere. It has been also found that the release of tritium solved in the bulk can be explained by diffusion models. The tritium release from the sub-surface layer, on the other hand, cannot be described by simple diffusion mechanisms. This is complicated by the concurrence and/or competition of the diffusion in the sub-surface layer and surface reactions, and then it is still under rigorous investigations.

As for Al_2O_3, it has been observed that the performance of gas chromatographic hydrogen isotope separation system is significantly impeded by adsorbed water, in other words under the presence of moisture in the isotopic mixture gas[5, 6]. This is considered due to the presence of OH-groups adsorbed on the carrier (commonly Al_2O_3 powder) of the working materials such as Pd-Pt alloy particles[5, 6]. In the separation column hydrogen isotopes in the loading mixture gas are firstly dissociatively absorbed by the working material and then released to gas phase as H_2, D_2 and T_2 according to thermodynamic isotope effect. Under the presence of OH-groups on the supporting Al_2O_3 powder, however, the dissolved hydrogen isotope atoms such as H, D, and T are spilled over to the support surface, where isotope replacement occurred with native H atoms of residual OH-groups[6]. This phenomenon caused severe interference on the isotope effect of hydrogen absorption/desorption by the working materials as Pd, Pd-Pt and so on[3, 4, 6]. Detailed mechanisms of the disturbance, however, have not been clarified so far. Since the presence of OH-groups on Al_2O_3 powder are unavoidable because the powder are exposed to the air even after rigorous out-gassing after the preparation, understanding of adsorption of water is also an important problem from this point of view.

As a first step to understand the tritium capture and release by/from the sub-surface layer as well as the supporting material, *ab initio* calculations were carried out for adsorption of H_2O on the surfaces of Cr_2O_3 and Al_2O_3, which were modelled by Me4O4 (Me = Cr or Al) clusters, by using Gaussian 03 package[10]. The aim of the present preliminary study is to figure out adsorption sites and species formed on the surfaces of Cr_2O_3 and Al_2O_3 exposed to H_2O vapor.

2. Modeling of Oxide Surfaces

Chromium oxide, Cr_2O_3, and aluminum oxide, α-Al_2O_3, belong to the tetragonal-hexagonal group, belonging to the space group of $R\bar{3}c$ (#167) structure, conventionally called as corundum

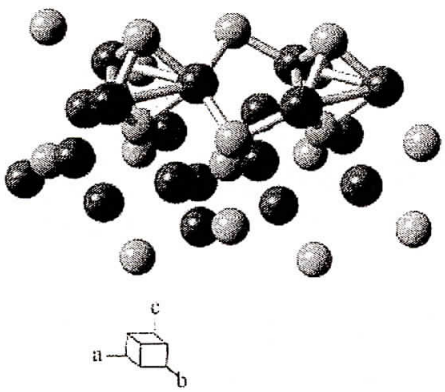

Fig. 1. A part of corundum unit cell, representing Me4O4 cluster frame ; dark balls represent Me atoms and light ones O atoms

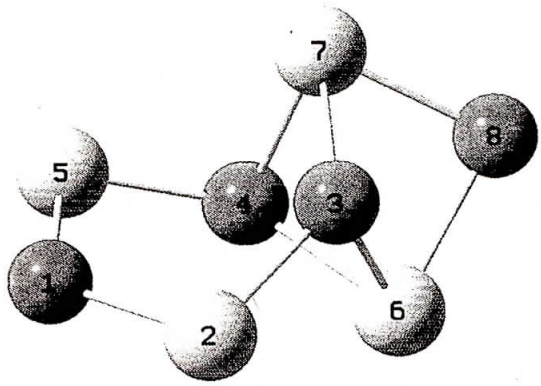

Fig. 2. Structure of the model cluster for Me4O4 (Me=Cr, Al); dark balls represent Me atoms and light ones O atoms

structure. The lattice parameters are $a = 4.9607$ and $c = 13.599$ Å for Cr_2O_3[11], and $a = 4.7589$ and $c = 12.991$ Å for α-Al_2O_3[12]. **Figure 1** demonstrates a part of the unit cell of corundum, for the sake of simplicity, where the blue balls represent metal atoms and the pink ones oxygen atoms. For inspecting the adsorption of H_2O on those oxide surfaces, it was required to simplify the structure for the sake of computing time by Gaussian 03. In the present study, small clusters consisting eight atoms were adopted for the structural optimization of adsorbed H_2O. **Figure 2** shows the cluster model of Me_2O_3 comprising four Me-atoms (Me= Al or Cr) and four O-atoms, where the atoms numbered 2, 5, 6 and 7 represent Me- atoms, and those of 1, 3, 4 and 8 are O-atoms. This is a characteristic configuration of atoms in the (001) palne of corundum structure as shown in **Fig.1**. **Tables 1 and 2** show the locations of atoms in the cartesian coordinate for Cr4O4 and Al4O4 clusters, respectively, where x, y and z values are in Å unit. These structures were fixed during the calculations of structure optimization for adsorption of H_2O, by assuming that the surfaces of those oxides are not subjected to relaxation owing to H_2O adsorption.

3. Structure Optimization

The *ab initio* structural optimization by Gaussian 03 was carried out by adding a H_2O molecule at an appropriate position of the Cr4O4 or Al4O4 cluster. In these cases, the cluster structures were fixed as mentioned above and the oxygen and two hydrogen atoms of water molecule were freed to move to find an optimum structure having minimum energy. The model chemistry and basis functions adopted for the structural optimization were UB3LYP of the density functional methods and Lanl2dz for Cr (or Al) and O with 6-31G(d,p) for hydrogen atoms, respectively. Owing to rather slow converging speed by personal computers used, the optimization started in low convergence criterion with the SCF option of conver=4

Table 1. Location of Cr and O atoms of Cr4O4 cluster in cartesian coordinate; x, y and z are given in Å

Atom	x	y	z
O	0.00000000	0.00000000	0.00000000
Cr	1.94580225	0.00000000	0.00000000
O	2.28131125	1.91665858	0.00000000
O	0.34900398	2.41164581	-1.71467835
Cr	-1.00415962	1.54951614	-0.61384818
Cr	2.32288731	2.02391144	-2.03345526
Cr	1.05445792	3.53366506	-0.16820509
O	2.43570260	4.00806037	-1.58781216

Table 2. Location of Al and O atoms of Al4O4 cluster in cartesian coordinate; x, y and z are given in Å

Atom	x	y	z
O	0.00000000	0.00000000	0.00000000
Al	1.85270356	0.00000000	0.00000000
O	2.21321318	1.81729010	0.00000000
O	0.34657297	2.34340857	-1.60909271
Al	-0.93486402	1.49186437	-0.57695793
Al	2.24103226	1.93922912	-1.96566465
Al	1.04286096	3.39843946	-0.09860491
O	2.36605368	3.84580421	-1.48731163

and proceeded further with the option of conver=8[13]. The optimization gives the structure of adsorbed species (adsorption sites, bond lengths and angles among respective atoms) and the total energy of the system. In the case of H_2O adsorption, the adsorption energy is evaluated as

$$E_{ads} = E_{tot}(\text{Me4O4-H}_2\text{O}) - E_{tot}(\text{Me4O4} + \text{H}_2\text{O}), \tag{1}$$

where E_{tot}(Me4O4-H_2O) is the total energy of the system obtained by the structure optimization and E_{tot}(Me4O4+H_2O) the total energy of Me4O4-H_2O (Me=Cr,Al) without optimization, where the H_2O molecule locates at 7 Å apart from a Me-atom, corresponding H_2O gas in the vacuum.

4. Results and Discussion

4.1. Adsorbed States of H_2O for Cr4O4

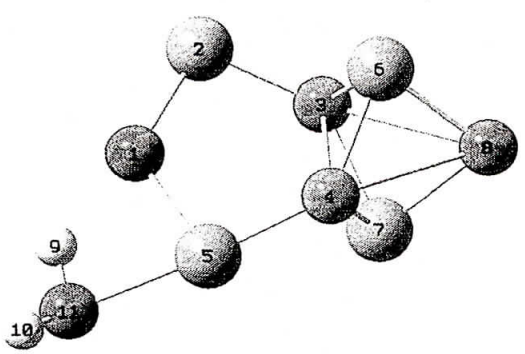

Fig. 3. Molecularly adsorbed species of H_2O for Cr4O4 cluster (Cr4O4-type-1)

Several kinds of adsorbed species were found and they could be roughly divided into five groups with respect to adsorption energy. The most weakly adsorbed species, $H_2O(a)$, showed the adsorption energy of -92.9 kJ/mol., whose structure is schematically shown in **Fig.3**, where the atoms numbered 1, 3, 4 and 8 are oxygen atoms, and those indicated as 2, 5, 6 and 7 chromium atoms of the Cr4O4 cluster; O(11), H(9) and H(10) constitutes H_2O moleclule in this case. The oxygen atom of H_2O molecule binds to the Cr(5) atom of the cluster. The bond length of Cr(5)-O(11) is 2.002 Å. This is slightly longer than the bond length of Cr(5)-O(1), 1.9458 Å, of the cluster frame. As for adsorbed H_2O molecule, the bond lengths of O(11)-H(9) and O(11)-H(10) are

1.005 and 0.965 Å and the angle ∠H(9)O(11)H(19) is 109.6 °. Although the structure of adsorbed $H_2O(a)$ was slightly deformed, the bond length and the bond angle of the adsorbed H_2O molecule was almost the same as those of free H_2O molecule (0.967 Å and 108.34 °), indicating that the interaction between Cr(5) and O(11) is weak enough. This type of adsorbed species is denoted as Cr4O4-type-1.

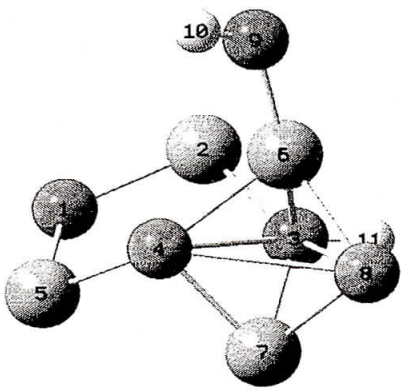

Fig. 4. Dissociatively adsorbed H_2O, forming Cr(6)-OH and O(3)-H bonds (Cr4O4-type-2)

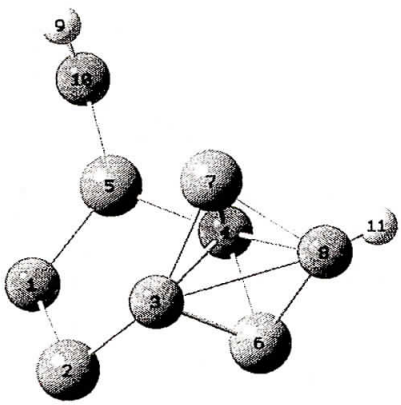

Fig. 5. Dissociatively adsorbed H_2O, forming Cr(5)-OH and O(8)-H bonds (Cr4O4-type-3)

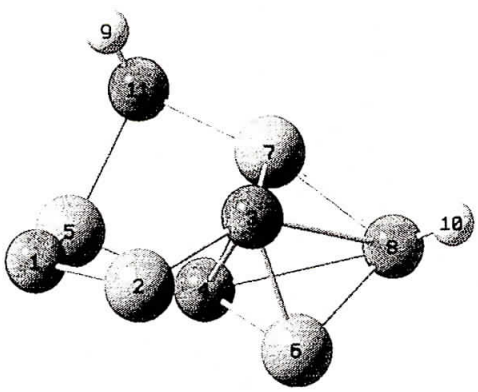

Fig. 6. Dissociatively adsorbed H_2O, forming Cr(5)Cr(7)-OH and O(8)-H bonds (Cr4O4-type-4)

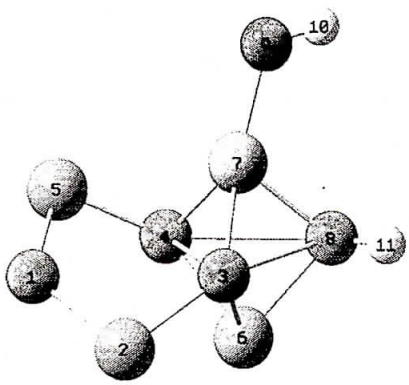

Fig. 7. Dissociatively adsorbed H_2O, forming Cr(7)-OH and O(8)-H bonds (Cr4O4-type-5)

Figure 4 illustrates schematic views of dissociatively adsorbed H_2O on the Cr4O4-cluster. It shows the formation of Cr(6)-O(9)H(10) and O(3)-H(11) bonds. In this case, O(9) corresponds to the oxygen atom of H_2O and O(8) does the one of Cr4O4 cluster. The bond length of Cr(6)-O(9) is 1.774 Å. The bond length of O(9)-H(10) is 0.967 and that of O(8)-H(11) 0.972 Å. The energy of adsorption was evaluated to be -168.2 kJ/mol. This type of adsorbed species is denoted as Cr4O4-type-2. **Figure 5**, which is denominated as Cr4O4-type-3 hereafter, also shows dissociatively adsorbed H_2O. In this case, the OH
fragment of H_2O bound to the Cr(5) atom. The bond length of Cr(5)-O(10) is 1.850 Å. Those

Table 3. Location of H and O atoms for Cr4O4-H_2O system in Z-matrix form

type/energy (kJ/mol)	atom1	atom2	length (Å)	atom3	angle (degree)	atom4	dihedral (degree)
Cr4O4-type-1 -92.9	H(10)	O(11)	0.965	Cr(5)	125.75	O(1)	-110.19
	H(9)	O(11)	1.005	Cr(5)	81.91	O(1)	-1.84
	O(11)	Cr(5)	2.002	O(1)	75.44	Cr(2)	-158.19
Cr4O4-type-2 -168.2	H(10)	O(9)	0.967	Cr(6)	122.74	O(4)	11.36
	O(9)	Cr(6)	1.774	O(4)	108.94	O(8)	-127.95
	H(11)	O(3)	0.972	Cr(6)	107.67	O(4)	-149.99
Cr4O4-type-3 -259.8	H(9)	O(10)	0.963	Cr(5)	130.68	O(1)	84.68
	O(10)	Cr(5)	1.850	O(1)	129.91	Cr(2)	-158.63
	H(11)	O(8)	0.967	Cr(7)	113.02	O(4)	73.68
Cr4O4-type-4 -297.9	H(9)	O(11)	0.976	Cr(5)	112.53	O(1)	-34.11
	O(11)	Cr(5)	1.923	O(1)	105.47	Cr(2)	-70.04
	O(11)	Cr(7)	2.089	Cr(5)	41.60		
	H(10)	O(8)	0.967	Cr(7)	114.84	O(3)	-72.22
Cr4O4-type-5 -338.1	H(10)	O(9)	0.966	Cr(7)	119.17	O(8)	1.31
	O(9)	Cr(7)	1.837	O(8)	111.04	O(3)	147.40
	H(11)	O(8)	0.967	O(3)	101.50	O(4)	-179.52

of O(10)-H(9) and O(8)-H(11) are is 0.963 and 0.967 Å, respectively. The adsorption energy was given as -259.8 kJ/mol. The thrid type of dissociatively adsorbed scecies is shown in **Fig.6**, where the oxygen atom of water binds to both Cr(5) and Cr(7) atoms. The bond lengths of O(11)-Cr(5) and O(11)-Cr(7) 1.923 and 2.089 Å, respectively. They are only slightly longer than the respective bond length of Cr4O4-type-3, 1.94580 Å. As for the lengh of OH bond, it was 0.976 for O(11)-H(9) and 0.967 Å for O(8)-H(10). The adsorption energy for this type was -297.9 kJ/mol. This type will be denoted as Cr4O4-type-4. The last type shown in **Fig.7** was found to be most stable with the adsorption energy of -338.1 kJ/mol. The oxygen atom of water binds to the Cr(7) with the bond length of 1.837 Å for O(9)-Cr(7), and those of O(10)-H(9) and O(8)-H(11) are 0.9665 Å and 0.9671 Å, respectively. This type is denominated as Cr4O4-type-5. The structures of adsorbed species for Cr4O4 cluster are summarized in **Table 3**.

4.3. Adsorbed States of H_2O for Al4O4

Adsorbed species of water for Al4O4 cluster can be roughly divided into four groups with respect to adsorption energy. Molecularly adsorbed species showed the smallest adsorption energy around -84 kJ/mol. **Figure 8** shows an example of molecularly adsorbed species. The oxygen atom of water molecule binds to Al(5) of the Al4O4 cluster, where the bond length of O(11)-Al(5) is 2.026 Å. This is considerably larger than that of O-Al (1.85270 Å) of Al4O4 cluster. In addition, the bond lengths of O(10)-H(9) and O(10)-H(11) in the adsorbed water molecule are 1.001 and 0.968 Å, and the angle $\angle$H(9)O(10)H(11) is 111.45°. Although these bond length and angle are slightly larger than those of free water molecule (0.967 Å and

108.34°), the bonding between O(11) and Al(5) does note affect noticeably to the structure of $H_2O(a)$ and then this could be recognized as molecularly adsorbed spcies. The energy of adsorption was calculated to be -91.6 kJ/mol. This species will be denoted as Al4O4-type-1.

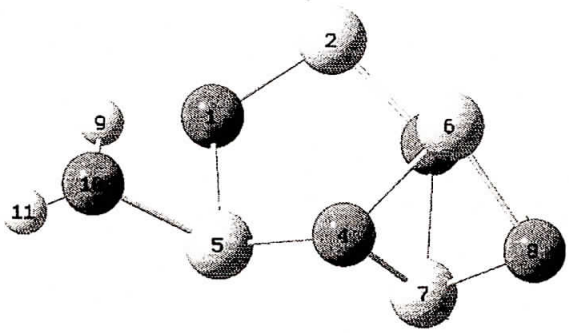

Fig. 8. Molecularly adsorbed species of H_2O for Al4O4 cluster (Al4O4-type-1)

The following figures are illustrations of dissociatively adsorbed species. They could be divided into three groups with respect to adsorption energy. **Figures 9 and 10** show typical examples of dissociatively adsorbed H_2O. The first type is the adsorption forming Al(7)Al(5)-OH (a)+O(3)-H (a) (**Fig.9**), and the second one Al(5)-OH (a)+O(3)-H (a) (**Fig.10**). These species are denoted as Al4O4-type-2 and Al4O4-type-3, respectively. For Al4O4-type-2, the bond length of

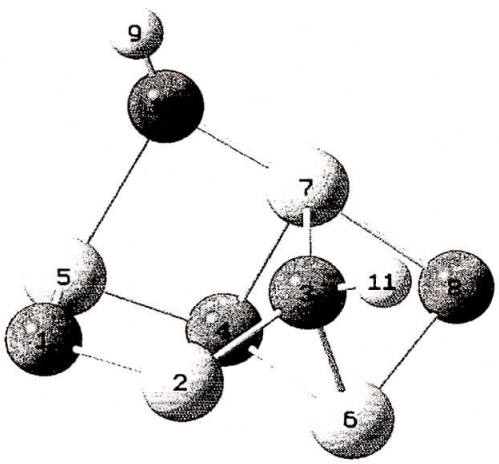

Fig. 9. Dissociatively adsorbed H_2O, forming Al(5)Al(7)-OH and O(3)-H bonds (Al4O4-type-2)

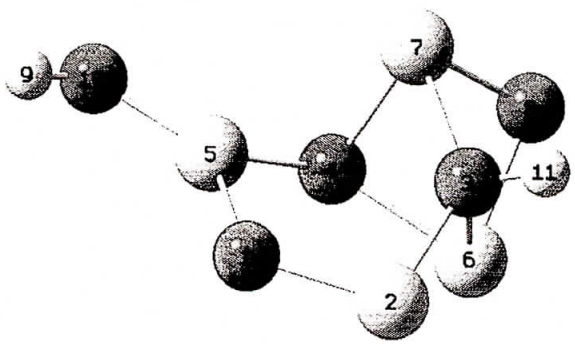

Fig. 10. Dissociatively adsorbed H_2O, forming Al(5)-OH and O(3)-H bonds (Al4O4-type-3)

Al(7)-O(10) (**Fig.9**) is 1.746 and that of O(10)-H(9) 0.963 Å. The O(10) atom also binds to Al(5) with slightly larger distance (2.221 Å) than that of Al(7)-O(10). The length of O(3)-H(11) is 0.976 Å. The adsorption enegy was evaluated to be -206.7 kJ/mol. The Al4O4-type-3 is different from Al4O4-type-2 in the adosprion site (**Fig.10**), although the adsorption energy of -209.2 kJ/mol was obtained for this species, being almost the same as that of Al4O4-type-2. In this case, the O(11) atom of OH group makes bonding only with Al(5) with the length of 1.692 Å for O(10)-Al(5). With respect to H(11)-O(3) bond, the distance between these atoms is 0.976 Å. **Figure 11** shows another kind of bridged type dissociative adsorption of water. The O(10) atom of the OH-group also binds to Al(7) and Al(5), but the bond lenghts of O(10)-Al(7) and O(10)-Al(5) are 1.819 and 2.036 Å, respectively, begin different from those

of Al4O4-type-2. In addition, the H atom of water binds to O(1) with the bond length of 0.967 Å. The adsorption energy was given as -254.4 kJ/mol. This type will be called as Al4O4-type-4. **Figure 12** is the schematic representation of the dissociatively adsorbed species having larger adsorption energy of -369.9 kJ/mol. In this case the oxygen atom of water binds to Al(7) with the length of 1.690 Å and the length of O(10)-H(11) is 0.960 Å. The dissociated H atom binds to O(8) atom of the length at 0.965 Å. This type is designated as Al4O4-type-5. Those structures of adsorbed species obtained for Al4O4 cluster are summarized in **Table 4.**

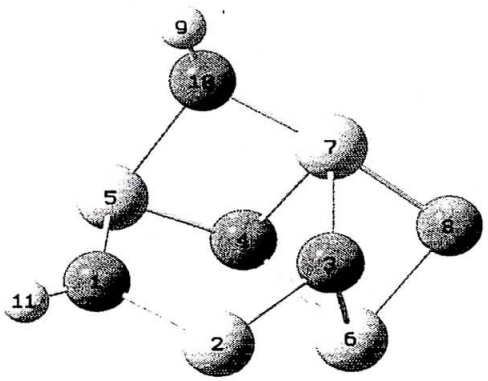

Fig. 11. Dissociatively adsorbed H_2O, forming Al(5)Al(7)-OH and O(1)-H bonds (Al4O4-type-4)

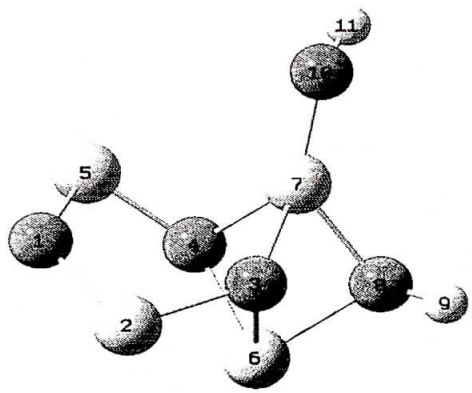

Fig. 12. Dissociatively adsorbed H_2O, forming Al(7)-OH and O(8)-H bonds (Al4O4-type-5)

Table 4. Location of H and O atoms for Al4O4-H_2O system in Z-matrix form

type/energy (kJ/mol)	atom1	atom2	length (Å)	atom3	angle (degree)	atom4	dihedral (degree)
Al4O4-type-1 -91.6	H(11)	O(10)	0.968	Al(5)	126.58	O(1)	118.72
	H(9)	O(10)	1.001	Al(5)	87.17	O(1)	3.93
	O(10)	Al(5)	2.026	O(1)	79.30	O(4)	117.58
Al4O4-type-2 -206.7	H(9)	O(10)	0.963	Al(7)	136.12	Al(5)	152.64
	O(10)	Al(7)	1.746	Al(5)	52.76	O(4)	158.79
	O(10)	Al(5)	2.221	Al(7)	38.76		
	H(11)	O(3)	0.976	O(8)	85.74	O(4)	175.45
Al4O4-type-3 -209.2	H(9)	O(10)	0.960	Al(5)	126.94	O(1)	6.14
	O(10)	Al(5)	1.692	O(4)	126.55	O(3)	148.47
	H(11)	O(3)	0.976	O(4)	145.44	O(8)	-3.66
Al4O4-type-4 -254.4	H(9)	O(10)	0.964	Al(7)	132.82	Al(5)	155.20
	O(10)	Al(7)	1.819	Al(5)	46.84	O(4)	156.53
	O(10)	Al(5)	2.036	Al(7)	40.68		
	H(11)	O(1)	0.967	Al(5)	120.60	O(4)	-149.80
Al4O4-type-5 -369.9	H(11)	O(10)	0.960	Al(7)	131.00	O(8)	52.13
	O(10)	Al(7)	1.690	O(8)	133.47	O(4)	-139.03
	H(9)	O(8)	0.966	O(3)	102.97	O(4)	-178.34

4.4. Inspection of *ab initio* calculations by TDS spectra of H_2O for Al_2O_3

The *ab initio* calculations described above showed that several different types of adsorption are possible for both Cr_2O_3 and Al_2O_3. However, there appeared no simple straightforward relations between the energy of adsorption and structure of adsorbed species. It appears, especially for dissociative adsorption, that the adsorption energy largely change with the site of binding of oxygen in dissociated OH-group and that of fragemt H adsorption. This feature might be due to the cluster models as well as the model chemistry and basis functions used adopted in the present study. With this respect, the above mentioned *ab initio* calculations should be examined with experimental results to inspect the reliability of calculalations. Thermal desorption spectra (TDS) are useful for this purpose.

Desorption of an adsorbed species from a surface under continuous pumping can be described as

$$N(t) = V(\frac{dP(t)}{dt}) + SP(t), \tag{2}$$

where $N(t)$ is the desorption rate and $P(t)$ the pressure in the system having the volume of V at time t; S is the pumping speed of the system. In the extreme case of $V(dP/dt) \ll SP$, the equation can be simplified as

$$N(t) = S\,P(t), \tag{3}$$

and then $P(t)$ is proportional to $N(t)$, providing the change in $N(t)$ with time. The desorption rate, $N(t)$, is described as

$$N(t) = -\frac{d\,n(t)}{dt} = \nu\, n(t)^{\alpha}\ \exp[-E_d/RT], \tag{4}$$

where $n(t)$ is the number of adsorbed molecules at time t, ν the frequency factor, E_d the activation energy for desorption, α the order of reaction, R the gas constant and T the temperature. Thermal desorption spectra are observed when the sample is heated with a function of time. In the case of linear temperature ramp, i.e., $T = T_0 + \beta\, t$, where T_0 is the starting temperature, β the rate of temperature rise, and t the time, a desorption peak appears at T_p that is given as

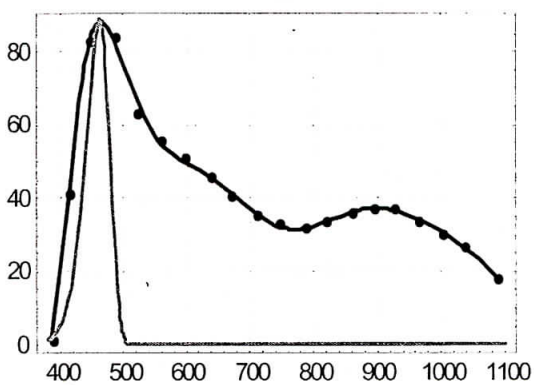

Fig. 13. Thermal desorption spectrun of H_2O from as-recieved γ-alumina; the bold line demonstrates the observed and thin line does the first order calculated spectrum for the first peak with $\nu = 2.0 \times 10^8$/sec and $E_d = 91.6$ kJ/mol.

$$\frac{E_d}{RT_p^2} = (\frac{\nu}{\beta})\exp[-\frac{E_d}{RT_p}] \tag{5}$$

$$= (\frac{\nu\, n_0}{\beta})\exp[-\frac{E_d}{RT_p}] \tag{6}$$

T_p is the peak temperature and n_0 the number of adosrbed molecule initially present. Eqs.(5) and (6) are valid for the first order and the second order desorption, respectively.

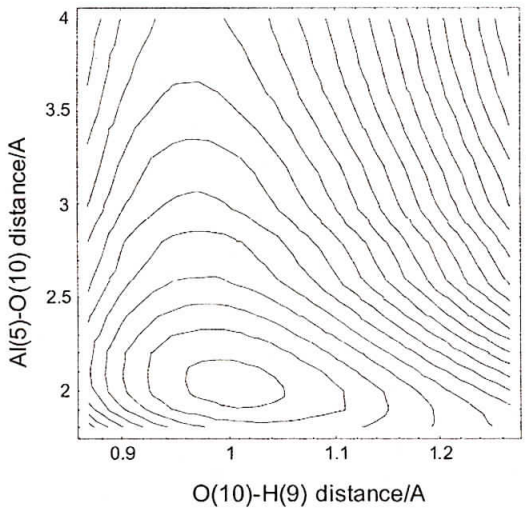

Fig. 14. PES (Potential Energy Surface) for H_2O-Al4O4-type-1; the difference in the level of countour lines is 0.1 eV

Figure 13 shows a desorption spectrum of water observed for as-recieved γ-alumina with a temperature ramp of 10 K/min.[5], where the abscissa represents the temperature in K, and the ordinate the signal intensity of m/e =18 of mass spectrometer in arbitrary unit. The circles and bold line show the observed desorption curve of H_2O. There arised three peaks about 500, 600 and 900 K. Since details of the measurement, i.e., the volume and pumping speed, are not known, it is assumed here that the pumping speed was large enough to validate Eq.(3). Although this should not be true, qualitative analysis could be done under this assumption. On account of the *ab initio* calculations, the first peak ascribed to moleculary adsorbed water and then this should obey the first order desorption kinetics. Accordingly the activation energy, E_d, could be estimated from Eq.(5) by adopting the frequency factor to be $\nu = 10^{13} \sim 10^{14}$/sec as commonly accepted. The value thus obtained was $130 \sim 140$ kJ/mol. The thin line in **Fig.13** is the desorption spectrum fitted to the observed one by by setting $\alpha = 1$, $\nu = 2.0 \times 10^8$/sec, $T = 293 + 10\,t$ and E_d= 91.6 kJ/mol. for Eq.(4). In this case, the activation energy for desorption was assumed to be the same as the energy of molecular adsorption evaluated the *ab initio* calculation. To examine the validity of this assumption, PES (Potenrial Energy Surface) was calculated by varying the distance of O(10)-H(9) and that of O(10)-Al(5) corredponding to **Fig.8**. The result is shown in **Fig.14**, where the abscissa represents the distance of O(10)-H(9) and the ordinate that of O(10)-Al(5) in Å unit. There appeared no noticeable suddle point. Hence the activation energy for desorption can be safely assumed the same as the adsorption energy for Al4O4-type-1. However, the values 91.6 kJ/mol. and 2.0×10^8/sec. for E_d and ν, respectively, are too small incomparison with those obtained from the conventional TDS analsys. In addition, the calculated desorption peak is too narrower than the observed first peak. With respect to the considerabley narrower peak, it should be mentioned that other types of molecularly adsorbed water with different adsorption energies can be exist on different crystal planes. It should be also mentioned that the peak boardening could arise from the $V\,dP/dt$ term in Eq.(2), which causes a desorption peak in "$N(t) - t$" to be weakened and broadened, especially at the tailing part of "$P(t) - t$" spectrum.

As for the fairly small value of ν for calculated desorption spectrum arises from the small value of E_d. It appears due to the model chemistry and basis functions used as well as cluster size. It should be also mentioned that the observed spectrum was obtained for γ-alumina,

whereas the calculation was done for α-alumia. Further examinations accounting those factors are needed in addition to much well defined TDS measurements.

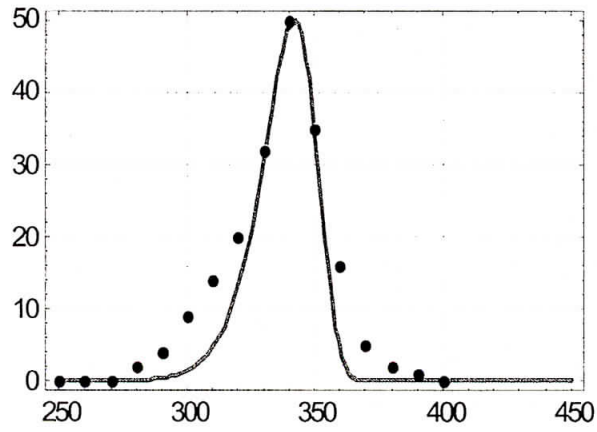

Fig. 15. Thermal desorption spectrun of H_2O from α-Cr_2O_3; the dots were read from Henderson's report[14] and thin line are the first order calculated spectra with $\nu = 3 \times 10^{13}$ and E_d = 92.9 kJ/mol.,respectively.

Figure 15 is a desorption spectrum of water from α-Cr_2O_3 surface (001) at a temperature ramp of 2 K/sec after the water exposure of 8.9 $\times 10^{14}$ molecules/cm^2 at 120 K, where the dots were the data points read from the paper by Hernderson and Chambers[14]. But the abscissa is in arbitrary unit, since the paper gives it as signal intensity of m/e=18 of mass spectrometer. The peak temperature, however, was invariant with the amount of exposure, and hence the desorption obeys the first order kinetics. The best values to reproduce the desorption peaks shown in their paper were reported to be $\nu = 10^{12}$/sec and E_d = 89 kJ/mol. The adsorption energy of -92.9 kJ/mol. obtained in the present study for the molecular adsorption is quite close to the value of 89 kJ/mol. for E_d. Then the peak was analyzed by applying E_d = 92.9 kJ/mol. in the same way as the first peak of water for alumina as mentioned above. The solid line in the figure is the calculated spectrum assuming that the frequency factor and activation energy for desorption are 3×10^{12}/sec and 92.9 kJ/mol, respectively, where the activation energy was assumed to be the same as the adsorption energy for molecular species evaluated for Cr4O4-cluster (see **Table.3**). According to a preliminay calculation of vibration, the stretching vibration of the H_2O molecule corresponding to the desorption was evaluated to be around 10^{12}/sec for this species. The figure shows that the calculated spectrum coincided unexpectedly well with the observed one. It should be mentioned here that the values of 89 kJ/mol (E_d) and $\nu = 7 \times 10^{12}$ reported in their paper[14] almost exactly overlaps with the solid line in this figure. The slight disagreement at the front part of the peak is due to the presence of another kind of desorption species[14]. As for the disagreement in the tailing part, it should be ascribed to the contribution of $V(dp/dt)$ term in Eq.(2), although the V/S ratio appears quite small in this case. These results indicate that the *ab initio* calculations for small clusters are valid as far as the molecular adsorption of water on (001) surface of α-Cr_2O_3 concerned. With respect to other species appeared in their paper, inspection of calculated absorption energies could not be done owing to the lack of data such as the H_2O pressure, volume and pumping speed of the system as well as the number of molecules desorbed. However, the calculated adsorption energies for other adsorbed species are considered meaningfull.

As for the calculated results for α-alumina, calculations for small clusters are considered also

meaningfull by accouning that the bond strength of Cr-O is not so much different from that of Al-O[15], suggesting that the adsorption energies for Cr_2O_3 do not differ much from those for Al_2O_3, being consistent with the results that similar adsorption energies were obtained between Cr4O4 and Al4O4 clusters. More detailed *ab initio* studies, however, should be carried out for adsorption/desorption kinetics along with observations of adsorption/desorption processes. Concerning the relation between the structure of adsorbed species and the adsorption energy, effects of different model chemistry and basis functions should be examined in detail. In addition, studies on larger clusters are also required on account of the size effect on this kind of calculations[16, 17, 18, 19], by which the structure as well as the energy of the system vary with cluster size.

5. Conclusions

A prelimiary *ab initio* study was carried out for adsorption of water on Cr_2O_3 and Al_2O_3 surfaces by adopting small clusters as Me4O4 (Me=Cr,Al) by use of Gaussian 03 package. The Me4O4 clusters were embraced by assuming (001) surfaces of Cr_2O_3 and Al_2O_3. It was found for both of the clusters that molecluar and dissociative adsorption take place, where the molecular adsorption preferentially occurs on a Me atom and the dissociative adsorption takes place through forming Me(or Me2)-OH + O-H bonds. In the latter case, one kind of -OH bonding is an on-top type and the other is a bridged type. Adsorbed water could be roughly divided into five groups for the Cr4O4 cluster and four groups for Al4O4 cluster with respect to the adsorption energy. There appeared a feature that the bond length between Me atom(s) and O atoms of water increases in the order of Me-OH (on-top) < Me2-OH (bridged) < Me-OH2 (molecular adsoption). But no straighforward simple relations could not be found between the structure of adsorbed species and adsorption energy.

Adsorption energies given by the *ab initio* calculations were examined through the analysis of thermal desorption spectra of H_2O for γ-alumina and (001) surface of α-Cr2O3. Although the TDS spectra for alumina could not be well explained by the cluster calculations, it can be ascribed to the fact that the TDS spectrum was observed for γ-alumina, whereas the calculation was done for α-alumina. In addition, it is considered that the model chemistry and basis functions as well as the cluster size were inadequate for this system. On the other hand, the TDS specrum for α-Cr_2O_3 could be quite well reproduced by use of the calculated adsorption energies.

However, detailed features could not be consistent between the calculated energies and the results of TDS analysis. One of the reasons is the TDS spectra used, which were not $N(t) - t$ curves but $P(t) - t$ curves, on accounting the signal intensity of m/e =18 to be proportional to water pressure. Another reason might be the calculations that were carried out for small cluster as Me4O4 (Me = Cr or Al). Effects of model chemistry and basis function should be examined and also the size effect on this kind of calculations should be studied to clarify relations between

structure of adsorbed species and adsorption energy as well as kinetic processes.

Acknowledgement

This work was partially supported by a Grant-in-Aid for Scientific Reserach on Priority Areas, 476, Tririum Science and Technology for Fusion Reactors, The MEXT.

References

[1] Y. Hatano, T. Maetani, and M. Sugisaki, *Fusion Technol.*, 28 (1955) 1182

[2] J. E. Castle and C. R. Clayton, *Corrosion Sci.*, 17 (1997) 7

[3] K. Watanabe, M. Matsuyama, T. Kobayashi, and A. Sakamoto, *Ann. Rept. Hydrogen Isot. Res. Ctr.*, 16 (1996) 33

[4] K. Watanabe, M. Matsuyama, T. Kobayashi, and W. M. Shu, *Fusion Engn. Design*, 39-40 (1998) 1001

[5] Y. Sakamoto, *BS thesis, Department of Chemistry, Fucaluty of Science, Toyama Univ.*, 1992

[6] T. Kobayashi, *MS Thesis, Department of Chemistry, Fucaluty of Science, Toyama Univ.*, 1993

[7] Y. Torikai, R-D. Penzhorn, M. Matsuyama, and K. Watanabe, *Fusion Sci. Technol.*, 48 (2005) 177

[8] Y. Torikai, M. Murata, R-D. Penzhorn, K. Akaishi, K. Watanabe, and M. Matsuyama, *J. Nucl. Mater.*, 363-365 (2007) 462

[9] R.-D. Penzhorn, Y. Torikai, M. Matsuyama, and K. Watanabe, *J. Nucl. Mater.*, 353 (2006) 66

[10] M. J. Frisch, G. W. Trucks, H. B. Schlegel, G. E. Scuseria, M. A. Robb, J. R. Cheeseman, Jr. J. A. Montgomery, T. Vreven, K. N. Kudin, J. C. Burant, J. M. Millam, S. S. Iyengar, J. Tomasi, V. Barone, B. Mennucci, M. Cossi, G. Scalmani, N. Rega, G. A. Petersson, H. Nakatsuji, M. Hada, M. Ehara, K. Toyota, R. Fukuda, J. Hasegawa, M. Ishida, T. Nakajima, Y. Honda, O. Kitao, H. Nakai, M. Klene, X. Li, J. E. Knox, H. P. Hratchian, J. B. Cross, C. Adamo, J. Jaramillo, R. Gomperts, R. E. Stratmann, O. Yazyev, A. J. Austin, R. Cammi, C. Pomelli, J. W. Ochterski, P. Y. Ayala, K. Morokuma, G. A. Voth, P. Salvador, J. J. Dannenberg, V. G. Zakrzewski, S. Dapprich, A. D. Daniels, M. C. Strain, O. Farkas, D. K. Malick, A. D. Rabuck, K. Raghavachari, J. B. Foresman, J. V. Ortiz, Q. Cui, A. G. Baboul, S. Clifford, J. Cioslowski, B. B. Stefanov, G. Liu, A. Liashenko,

P. Piskorz, I. Komaromi, R. L. Martin, D. J. Fox, T. Keith, M. A. Al-Laham, C. Y. Peng, A. Nanayakkara, M. Challacombe, P. M. W. Gill, B. Johnson, W. Chen, M. W. Wong, C. Gonzalez, and J. A. Pople, *Gaussian03, RevisionB.03*, Gaussian Inc.and Pittsburgh, 2003

[11] *JCPDS-JCDD, pdf-84-1616*

[12] *JCPDS-JCDD, pdf-81-2267*

[13] Æleen Frisch, Micahel J. Frisch, and Gary W. Trucks, *Gaussian03 User's Reference.* Gaussian Inc. Carnegie, PA 15106 USA, 2003

[14] Michael A. Henderson and Scott A. Chambers, *Surface Sci.*, 449 (2000) 135

[15] In R. C. Weast, editor, *CRC Handbook of Chemistry and Physics, 62nd ed.* The Chemical Rubber Co., 1971

[16] R. Broer, I. P. Bartra, and P. S. Gagus, *Phil. Mag. B*, 51 (1985) 243

[17] E. M. Fernarndez, R. I. Eglitis, G. Borstel, and L. C. Balbas, *Comp. Mater. Sci.*, 39 (2007) 587

[18] E. Penev, P. Kratzer, and M. Scheffler, *J. Chem. Phys.*, 110 (1999) 3986

[19] S. Erkoc, T. Bastug, M. Hirata, and S. Tachimori, *Chem. Phys. Letters*, 321 (2000) 321